The application of multiscale modelling to the process of development and prevention of stenosis in a stented coronary artery

D.J.W Evans, P.V Lawford, J Gunn, D Walker, D.R Hose, R.H Smallwood, B Chopard, M Krafczyk, J Bernsdorf and A Hoekstra

Supplementary data	"Data Supplement" http://rsta.royalsocietypublishing.org/content/suppl/2009/02/17/366.1879.3343.DC1.html
References	**This article cites 46 articles, 16 of which can be accessed free** http://rsta.royalsocietypublishing.org/content/366/1879/3343.full.html#ref-list-1
Rapid response	Respond to this article http://rsta.royalsocietypublishing.org/letters/submit/roypta;366/1879/3343
Subject collections	Articles on similar topics can be found in the following collections computer modelling and simulation (45 articles)
Email alerting service	Receive free email alerts when new articles cite this article - sign up in the box at the top right-hand corner of the article or click **here**

The application of multiscale modelling to the process of development and prevention of stenosis in a stented coronary artery

By D. J. W. Evans[1,*], P. V. Lawford[1], J. Gunn[2], D. Walker[3],
D. R. Hose[1], R. H. Smallwood[3], B. Chopard[4], M. Krafczyk[5],
J. Bernsdorf[6] and A. Hoekstra[7]

[1]*Academic Unit of Medical Physics,* [2]*Cardiovascular Research Unit, and*
[3]*Department of Computer Science, University of Sheffield,*
Sheffield S10 2TN, UK
[4]*Computer Science Department, University of Geneva,*
Geneva 1211, Switzerland
[5]*Institute for Computer Applications in Civil Engineering, Technical University*
of Braunschweig, Braunschweig 38106, Germany
[6]*NEC Laboratories Europe, NEC Europe Ltd., Sankt Augustin 53757, Germany*
[7]*Computational Science, University of Amsterdam,*
Amsterdam 1018, The Netherlands

The inherent complexity of biomedical systems is well recognized; they are multiscale, multiscience systems, bridging a wide range of temporal and spatial scales. While the importance of multiscale modelling in this context is increasingly recognized, there is little underpinning literature on the methodology and generic description of the process. The COAST (complex autonoma simulation technique) project aims to address this by developing a multiscale, multiscience framework, coined *complex autonoma* (CxA), based on a hierarchical aggregation of coupled cellular automata (CA) and agent-based models (ABMs). The key tenet of COAST is that a multiscale system can be decomposed into *N* single-scale CA or ABMs that mutually interact across the scales. Decomposition is facilitated by building a scale separation map on which each single-scale system is represented according to its spatial and temporal characteristics. Processes having well-separated scales are thus easily identified as the components of the multiscale model. This paper focuses on methodology, introduces the concept of the CxA and demonstrates its use in the generation of a multiscale model of the physical and biological processes implicated in a challenging and clinically relevant problem, namely coronary artery in-stent restenosis.

Keywords: complex automata; multiscale modelling; scale separation map; restenosis

* Author for correspondence (david.evans@sheffield.ac.uk).

1. Multiscale modelling and simulation in biomedicine

Recent advances in experimental techniques have created new insights into biomedical processes on many levels of detail. The complete cascade from individual components to a fully integrated biomedical system crosses many orders of magnitude in temporal and spatial scales (Sloot *et al.* 2006). We have access to data from virtually all levels between 'molecule' and 'man' and yet we have few models that enable us to study these processes as an integrated whole. The sequence from the genome, proteome, metabolome and physiome to health comprises multiscale, multiscience systems (Noble 2002; Finkelstein *et al.* 2004). Studying biological subsystems, their organization and their mutual interactions, through an interplay between laboratory experiments and modelling and simulation, should lead to an understanding of biological function and to a prediction of the effects of perturbations (e.g. genetic mutations or the presence of drugs; Di Ventura *et al.* 2006). The concept 'from genes to health' is the vision of the Physiome (Hunter *et al.* 2006) and the ViroLab (Sloot *et al.* 2006) projects, where multiscale modelling and simulation of the aspects of human physiology are the ultimate goal.

Modelling biomedical systems is a challenging problem but has the potential to improve our understanding of key interactions. The inherent complexity of biomedical systems is now beginning to be appreciated fully; they are multiscale, multiscience systems, covering a range of phenomena from molecular and cellular biology, via physics and medicine, to engineering, and crossing many orders of magnitude with regard to temporal and spatial scales (Smye & Clayton 2002; Quarteroni & Veneziani 2003).

Despite the widely acknowledged need for multiscale modelling and simulation, there is a scarcity of underpinning literature on the methodology and generic description of the process. There are many excellent papers that present multiscale models (including many with important biomedical applications; Noble 2002; Hunter & Nielson 2005), and some specialized journals exist (e.g. *Multiscale Modeling and Simulation, International Journal on Multiscale Computational Engineering*), but few methodological papers on multiscale modelling have appeared (Ingram *et al.* 2004; Weinan *et al.* 2007).

The COAST (complex autonoma simulation technique) project (www.complex-automata.org) aims to fill this gap by developing a multiscale, multiscience framework, coined *complex autonoma* (CxA), for modelling and simulation of complex systems, based on a hierarchical aggregation of coupled cellular automata (CA; Masselot & Chopard 1998; Ilachinski 2001) and agent-based models (ABMs; Wooldridge 2002; Walker *et al.* 2004). CxA were recently proposed by us as a paradigm for modelling multiscale complex systems (Hoekstra *et al.* 2007). The key tenet of COAST is that a multiscale system can be decomposed into N single-scale CA or ABMs that mutually interact across the scales. Decomposition is facilitated by building a scale separation map (SSM) on which each single-scale system can be represented as an area according to its spatial and temporal scales. Processes having well-separated scales are easily identified as the components of the multiscale model. COAST will validate the CxA approach by applying it to the challenging clinical problem of coronary artery in-stent restenosis (ISR).

This paper introduces the concept of the CxA and demonstrates its use in the generation of a multiscale model of the physical and biological processes implicated in tissue regrowth after stent deployment. The focus is on the
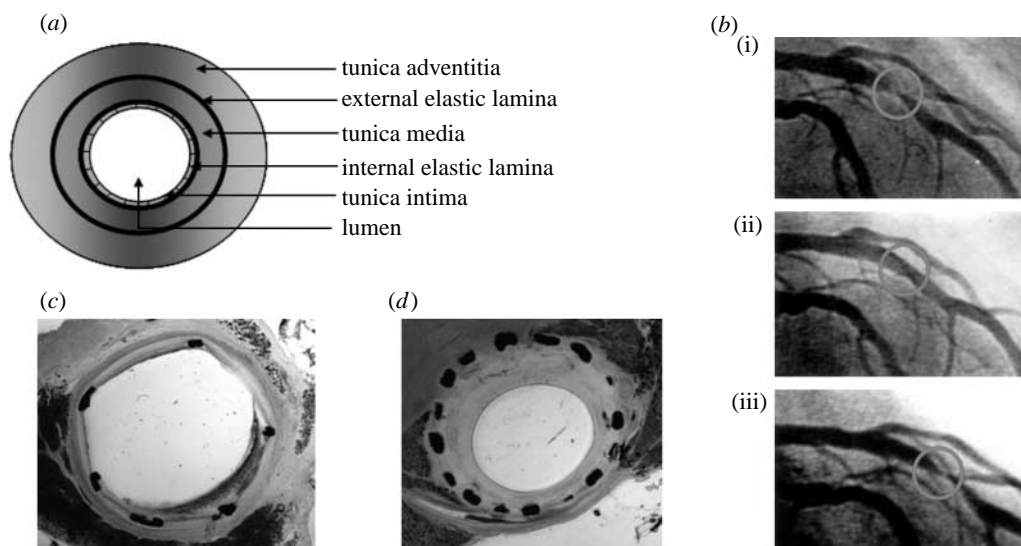
Figure 1. Background to arterial structure and stenting. (*a*) Schematic highlighting the different layers (tunica) of the vessel wall. The intima comprises a single layer of endothelial cells (ECs) that serves to maintain a biologically neutral interface between blood and tissue. The media comprises largely smooth muscle cells (SMCs) that function to oppose the forces exerted on the artery by pulsatile blood flow through the lumen. This layer is dynamic in nature and can contract or relax in response to chemical signals. The adventitia contains many blood vessels that provide a blood supply to the cells within the vessel wall. The main cell type in this layer is the fibroblast. These cells secrete extracellular matrix. (*b*) (i) Angiogram depicting a stenosed coronary artery pre-intervention (circled). (ii) Blood flow to the myocardium is then restored following intervention, which might include stent deployment (circled). (iii) Six months post-intervention the artery has restenosed (circled). Angiograms courtesy of J. Gunn, University of Sheffield. (*c*) Section from a porcine artery, 28 days post-stenting (minimal neointima). (*d*) Section from a porcine artery, 28 days post-stenting (significant neointima).

methodology used for the development of the model rather than on its results. Model validation will entail the use of a porcine dataset (Malik *et al.* 1998; Dean *et al.* 2005). This fully documented histological archive comprises hundreds of arterial sections (figure 1*c,d*) of stented porcine arteries. The morphological and physiological information derived from the analysis of these sections will allow a quantitative measure to be applied to a biological rule set for ISR based on an extensive literature review.

2. Background to the system to be modelled: angioplasty, stenting and restenosis

Coronary artery disease refers to the accumulation of atheromatous plaque within the wall of the coronary arteries. The reported presence of fatty streaks in the walls of coronary vessels in children is consistent with the chronic nature of disease progression (Napoli *et al.* 1997). An atherosclerotic plaque typically consists of a lipid-rich core within an eccentrically thickened intima (for artery

structure, see figure 1*a*). The central lipid-rich core of the typical lesion contains many lipid-laden foam cells that are derived from blood monocytes (Klurfeld 1985). Enlargement of such a lesion can lead to stenosis (narrowing) of the coronary artery and a decreased oxygen supply to the heart.

Coronary heart disease remains the most common cause of death in the UK, being responsible for approximately 105 000 deaths in 2004 (BHF 2007). Percutaneous coronary intervention represents one possible treatment strategy. This involves the advancement of a guidewire from the point of insertion (usually incision into the femoral artery at groin level), via the aorta, to the site of the stenosis within the coronary artery. An inflatable balloon can then be advanced along the guidewire and used to reopen the stenosed artery. Subsequently, a balloon-expandable metal frame (stent) may also be advanced along the guidewire and deployed to provide a scaffold, thus maintaining an open vessel lumen. In 2005, 94 per cent of 70 142 UK procedures involved the deployment of a stent (BCIS 2007). Unfortunately, restenosis remains a significant complication following stent deployment. This pathology can be described as 'a loss of gain', i.e. a late return of the vessel lumen to a size similar to that before intervention (figure 1*b*).

The stent serves as a mechanical scaffold, preventing vessel spasm or any long-term negative vessel remodelling (physical reduction in lumen/artery diameter), which was previously a complication of balloon angioplasty without stent deployment (Indolfi *et al.* 2003). Restenosis following stenting is largely a result of vascular smooth muscle cell (VSMC) proliferation (Mudra *et al.* 1997). In the latest generation of stents, the metal is coated with a polymer capable of releasing bound drugs at controlled rates with the purpose of limiting or preventing ISR. Administration of antiproliferative agents via drug-eluting stents has resulted in a reduced rate of clinical restenosis from approximately 10 per cent (with bare metal stents) to approximately 5 per cent. Despite this success, ISR remains an increasing and significant problem, given the ageing nature of the population (OECD 2007), the extension of stenting for use in challenging patient subsets (e.g. diabetic patients) and the global trend towards an increased use of stenting to treat coronary heart disease (Bernstein *et al.* 2003). Concerns regarding late thrombotic events (Carlsson *et al.* 2006; Leon & Stone 2006), combined with issues of cost-effectiveness (Eisenberg *et al.* 2006; Tezduyar *et al.* 2007) for drug-eluting stents, provide a rationale for the improvement of the existing, and the development of alternative, therapeutic strategies.

The majority of investigations consider the biological and physical processes important in the pathology of ISR independently, when, as will be discussed later, there is a complex interplay between the two. It is likely, therefore, that advances in our understanding of this complex pathophysiology, and strategies to prevent it, may be achieved via an approach that recognizes restenosis as a multiscience, multiscale phenomenon. The approach adopted in COAST should allow the investigation of key questions central to the pathology of ISR. The model could be used to investigate what drives the normal healing response to stent deployment past a threshold in certain individuals and not in others, or what factors are critical to halting restenosis. It will also provide a valuable tool for the study of drug elution.
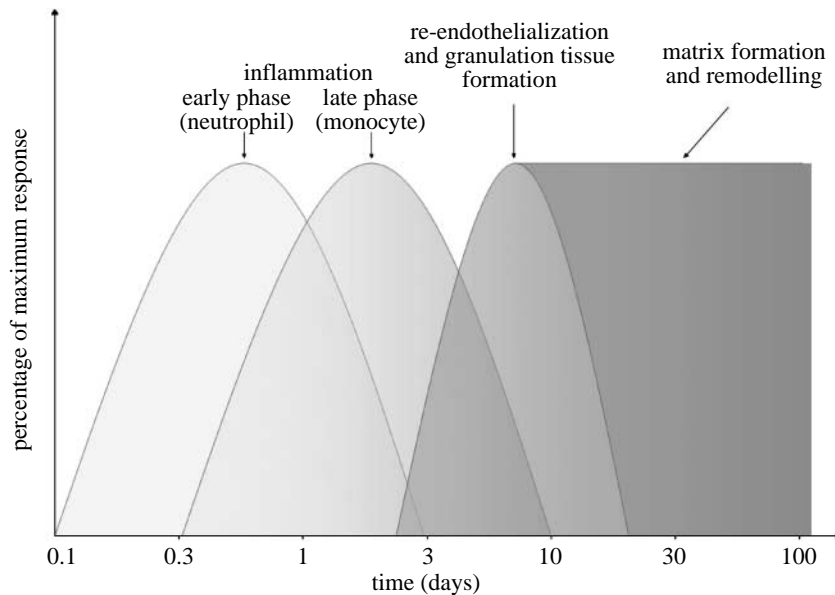
Figure 2. Schema of the classical wound healing response.

3. Identification of the key biological and physical processes

Before starting the process of constructing a multiscale model of a complex system, it is necessary to review the literature to identify the quantitative and qualitative data that are available, and what data are lacking. It can thus be established whether sufficient information exists to make the construction of the individual models feasible. Consideration of species and experimental design is important when sourcing data. As we will use a porcine dataset for validation purposes, where possible, data were obtained from studies employing porcine models. When such data were unavailable, then data from studies in humans or other species were considered. With regard to SSM construction, this scenario presents fewer problems in a qualitative sense than quantitatively; although there is significant homology between species with regard to the nature of the biological and physical processes involved in the generation of ISR, there are substantial differences with regard to the time-scales over which these processes occur.

We began our assessment of ISR by describing the process in a manner with which a biologist would be familiar. Restenosis can be considered to be a mani-festation of the classical wound healing response expressed specifically in vascular tissue (Forrester *et al.* 1991). This suggests categorization of the processes following the initial injury (i.e. stent deployment) into a number of stages. An initial biphasic inflammatory stage (i.e. involving the recruitment of leucocytes) is followed by a period of granulation (the formation of new connective tissue and capillaries), and finally by a period of extracellular matrix deposition and remodelling (figure 2). The main biological processes, key to the generation of a neointimal lesion (i.e. ISR), are summarized in the following

sections. The comprehensive review on which this is based, which we intend to publish in its entirety in the near future, is deliverable (www.complex-automata. org) from the COAST project.

(*a*) *Arterial injury and stent geometry*

Stent design and its geometrical consequences have a direct effect on the biological events observed in the vessel following deployment (Morton *et al.* 2004; Dean *et al.* 2005). In particular, strut thickness, number and cross-sectional shape, in combination with stent length, influence the symmetry of deployment and degree of injury/stretch; these, in turn, determine the amount of neointima that is formed.

(*b*) *The role of inflammation*

Areas in which the endothelium is damaged are rapidly lined by activated platelets. Leucocytes are able to interact transiently (roll) with adherent platelets before becoming stationary and adhering firmly. Both leucocyte rolling and firm adhesion are mediated by the interaction of adhesion molecules and their respective receptors on the leucocyte and platelet surfaces. Transmigration of the leucocyte into the vessel wall occurs in response to chemotactic agents. Once within the vessel wall (or neointima), leucocyte secretion of growth factors and cytokines drives smooth muscle cell (SMC) migration and proliferation, changes in extracellular matrix composition and further recruitment of leucocytes to the site of injury. These inflammatory events begin as beneficial reparative processes but may ultimately result in a detrimental vascular change, namely restenosis (Welt & Rogers 2002).

(*c*) *Platelet deposition and aggregation*

Despite contradictory evidence concerning the exact role of the platelets in neointimal proliferation and restenosis, it is apparent that many characteristics of this 'cell' type are consistent with a potential involvement (Bienvenu *et al.* 2001). Platelets adhere to the sites of vascular injury, such as those caused by the deployment of the stent, and secrete factors that both directly and indirectly stimulate VSMC proliferation and migration. Platelet activation results in the release of chemoattractant molecules and the upregulation of surface adhesion molecules, which allows interaction with other inflammatory cell types, thus homing them to the site of vascular injury (Yokoyama *et al.* 2005). Here, they too can release growth factors and cytokines initially to drive reparative processes that may eventually progress to pathophysiological status (i.e. restenosis).

(*d*) *Smooth muscle hyperplasia*

The degree of VSMC proliferation observed is dependent on the species, the model examined and the methods used to assess proliferation. Furthermore, an interrelationship between VSMCs and endothelial cells (ECs) governs the overall development of the neointimal lesion. The origins of SMCs within healthy arteries and vascular lesions are diverse (Zalewski *et al.* 2002; Sata 2003) and dependent on the nature of the injury preceding lesion development. One can postulate that a high degree of injury and loss of the endothelium may result in

a significant contribution from circulating bone marrow-derived cells. This would suggest that the process of stenting may result in a neointimal lesion derived from both a medial and a circulating VSMC source; however, this has yet to be confirmed.

(*e*) *Cell signalling*

Information received at the cell surface (e.g. by a growth factor interacting with a receptor) is transduced to the nucleus via several families of signalling molecules. Evidence supports a role for both mechanically and chemically induced activation of the phosphoinositide 3-kinase/Akt (PI3K/Akt) and extracellular signal-regulated kinase 1/2 signalling pathways in vascular cell proliferation, migration and survival. The transcription factor nuclear factor κB operates downstream of both of these pathways. Care needs to be taken when extrapolating data from *in vitro* studies, as the precise contribution of individual pathways and the relationship between pathway and cellular response is species and cell type specific (Goncharova *et al.* 2002). Activation of the PI3K/Akt pathway following stent implantation has also been observed *in vivo* (Zhou *et al.* 2003).

(*f*) *Remodelling*

The presence of a stent largely eliminates any long-term negative remodelling of a vessel as is observed following balloon angioplasty alone (Farb *et al.* 1999). However, alterations in the composition of the vessel wall do occur following percutaneous coronary intervention with stent deployment. Cytokine-driven extracellular matrix remodelling is a key feature following stent deployment and is necessary to facilitate SMC migration and proliferation. Matrix metalloproteinases (Ge *et al.* 2006) and plasminogen activators (Parfyonova *et al.* 2004) are key mediators of this remodelling, and some interplay occurs between these two families of proteases.

(*g*) *Flow, shear and cyclic strain*

Endothelial cells and VSMCs are exposed to shear stress and cyclic stretch, and are able to detect changes in these forces, transducing them via signalling cascades and gene expression to a cellular response tailored to alter vessel architecture in order to normalize these forces (Grimm *et al.* 2005; Haga *et al.* 2007). Shear stress is an important factor in determining a vessel's propensity to develop atherosclerosis and restenosis post-stenting. Modulation of shear stress due to stent deployment is important in determining the pattern and degree of restenosis observed. Oscillatory or disturbed flow and low wall shear stress are associated with atherogenesis and restenosis, whereas laminar flow and high wall shear stress are generally considered atheroprotective and thought to prevent the formation of neointima through inhibition of cell proliferation. Cyclic strain also influences EC and VSMC behaviours through the modulation of gene expression. The exact relevance of these changes in cellular behaviour to restenosis is much less well defined.

In summary, it is likely that individual cells respond to changes in extracellular mechanical forces in a manner that attempts to normalize these forces, thus supporting the notion that the vessel as a whole remodels in an attempt to
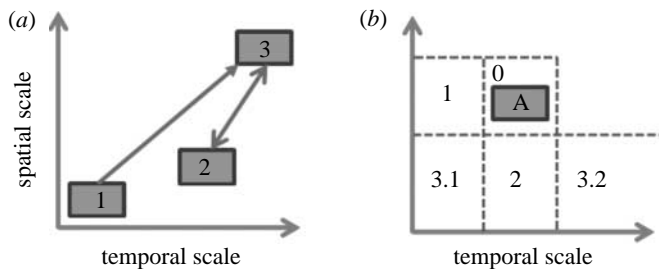
Figure 3. Scale separation diagrams. (*a*) Scale map showing three subsystems and an example of mutual couplings. (*b*) Interaction regions on the scale map.

normalize the forces experienced. The key physical parameters, namely flow, shear stress and cyclic strain, are inextricably linked with the biological processes responsible for triggering morphological changes, regardless of whether these changes are physiological or pathophysiological in nature. Stent designs that minimize the effects of stent deployment on these physical parameters should also reduce pathophysiological changes in vessel architecture, thus reducing ISR.

4. Scale separation

Having identified the key physical and biological processes central to the development of the restenotic lesion, quantitative data relating to the spatial and temporal characteristics of these processes were used to construct an SSM.

The SSM is a graphical representation of all single-scale subsystems that make up the full multiscale system in terms of their spatial and temporal scales, and in terms of their mutual coupling. By considering two mutually coupled processes on the SSM, five interaction regions are identified, each giving rise to specific multiscale coupling paradigms (Hoekstra *et al.* 2007). By applying the SSM concept to CxA, a methodology is introduced that allows one to place single-scale CA or ABMs unambiguously on the SSM, and to decide on the scale separation and interaction regions in which coupled processes fall. Processes having well-separated scales are easily identified as the components of the multiscale model.

The SSM is defined as a two-dimensional map, with the horizontal axis coding for temporal scales and the vertical axis for spatial scales. Each subsystem occupies a certain area on this map. Figure 3*a* shows an example of an SSM, in which three subsystems have been identified. Subsystem 1 operates on small spatial scales, and short temporal scales, subsystem 2 at intermediate scales and subsystem 3 at large scales. This could represent processes operating at the micro-, meso- and macroscales, for example.

After identifying all subsystems and placing them on the scale map, coupling between subsystems is then represented by directed edges on the map. The distance between subsystems on the map indicates which coupling paradigm should be used to simulate the overall system. In the worst case, the subsystems have significant overlap and one is forced to use the smallest scales everywhere. This would probably result in intractable simulations. On the other hand, if the subsystems are well separated and the smallest scale subsystems are in

equilibrium, then they can be solved separately, although infrequent (possibly event-driven) feedback between the subsystems will still be required. More details on this can be found in Hoekstra *et al.* (2007).

Consider two processes, A and B, each with their own spatial and temporal scales, denoted by ξ_i and τ_i, respectively, where $i \in (A, B)$. Assume that A has the largest spatial scale, or, in the case where the spatial scales are the same, A has the largest temporal scale. In other words, we have $(\xi_B < \xi_A)$ *or* $(\xi_B = \xi_A$ *and* $\tau_B < \tau_A)$. We can now investigate the different possibilities of placing B on the map relative to A. This leads to a classification of interaction regions, as shown in figure 3*b*. Depending on the location of B, we can identify the following interaction regions:

— *Region 0*. A and B overlap, and there is no scale separation.
— *Region 1*. Here $\xi_B = \xi_A$ *and* $\tau_B < \tau_A$, so we observe a separation of temporal scales at the same spatial scale.
— *Region 2*. Here $\xi_B < \xi_A$ *and* $\tau_B = \tau_A$, so we observe a separation in spatial scales like coarse and fine structures on the same temporal scale.
— *Region 3*. Separation in both temporal and spatial scales.

If B is located in region 3.1, this leads to the well-known situation of micro ⇔ macro coupling, with a fast process occurring on a small spatial scale (B) coupled to a slow process occurring on a large spatial scale. This type of multiscale model has received most attention in the literature, and the coupling paradigms explained earlier have mostly been applied in this region. When B is in region 3.2, we have the reverse situation: a slow process acting on a small spatial scale is coupled to a fast process acting on a large spatial scale. We believe that this is very relevant to the coupling of biological with physical processes, where a biological process, such as the slow response of cells, is coupled to a faster physical process on a larger scale (e.g. blood flow in arteries).

Note that we do not have to consider other regions of the scale map, because the roles of A and B are simply reversed, and we revert to one of the cases identified above.

The next step is to find the actual size of the processes on the SSM, quantify the scale separation and, based on this, decide on the type of multiscale coupling required. This, in combination with the fact that a CxA is built from single-scale CA or ABM, allows us to define generic multiscale coupling templates for each interaction region in figure 3*b*.

The concept of the SSM, as formalized by Hoekstra *et al.* (2007), is applicable to many other complex systems, for example, coral growth (Merks *et al.* 2003), thrombosis and snow transport/deposition (Masselot & Chopard 1998). Indeed, Fazekas *et al.* (2007) used SSMs in multiscale modelling and time-scale analysis of the human limb.

The main idea is that each CA or ABM (vertex of the CxA) can be expressed with a common instruction flow. This provides a way to identify the generic coupling templates as proposed above. We represent the workflow with a pseudo-code abstraction, termed the *submodel execution loop* (SEL) (table 1).

Although this pseudo-code uses the terminology of lattice gas simulation, it can be argued (see below) that the concepts are readily generalized to CA and ABM simulations. The CA or ABM operates on a computing domain D. For a

Table 1. The workflow with a pseudo-code abstraction, termed the *submodel execution loop* (SEL). (Note that in the SEL, operators are written in bold.)

```
D:=Dinit                    /* initialization of the domain */
f:=finit                    /* initialization of state variables */
t:=0                        /* initialization of time */
While Not EC
  t+=Δt                     /* increase time with one time step Δt */
  D:=U(D)                   /* update the domain */
  f:=B(f)                   /* apply boundary conditions */
  f:=C(f)                   /* collision, update state of cells */
  f:=P(f)                   /* propagation, sent information
                               to neighbours */
  Oi(f)                     /* compute observables from new state */
End
  Of(f)                     /* compute observables from final state */
```

CA, this is the lattice of (computational) cells and the boundaries, and for an ABM, the set of agents and the environment in which they reside. Each cell in a CA and agent in an ABM has a set of state variables f. At the start of the SEL, the domain and the state variables are initialized by the operators D_{init} and f_{init}, respectively. The simulation time t is set to an initial value (0 in this case). After initialization, the CA or ABMs enters into an iteration loop, whose termination is controlled by an end condition computed by EC. The end condition can simply be a fixed number of iterations, but could also be some convergence criterion depending upon the state variables. Within the main iteration loop, the time is first increased with a time-step Δt. Next, the domain is updated by the operator U. If the domain is static, this operator is simply the identity operator I. However, in many models, the domain is dynamic. For instance, in a CA, new cells can be created or the existing cells removed (e.g. due to the movement of the boundary), and in an ABM, agents can be created or destroyed, or the environment in which they reside can change. In all these cases, U will execute these domain updates. Next, the sequence $PCB(f)$ is executed (first boundary conditions, then collision and finally propagation). The terminology *collision–propagation* is borrowed from the lattice gas automata framework (Masselot & Chopard 1998). However, this is equivalent to the more classical *gather–update* CA paradigm. First, the operator B applies the boundary conditions. In a CA, this means that missing information is constructed, which is needed for the actual state updates by C (see below) of the cells lying at the boundary of the domain D. For instance, if the state variables represent a concentration of some species, the boundary condition could specify a flux of those species into the domain, and from that, missing information on the domain boundary cells is computed. In an ABM, the operator B could also represent a boundary condition on the environment in which the agents live (e.g. again the influx of some species), but it could also represent the interaction with agents outside the domain D (and therefore not explicitly simulated). Next, the actual state change of all cells in a CA or agents in an ABM is computed by the collision operator C. Finally, information is sent to neighbouring cells or agents by the propagation operator P. The CA or ABM is now updated for the
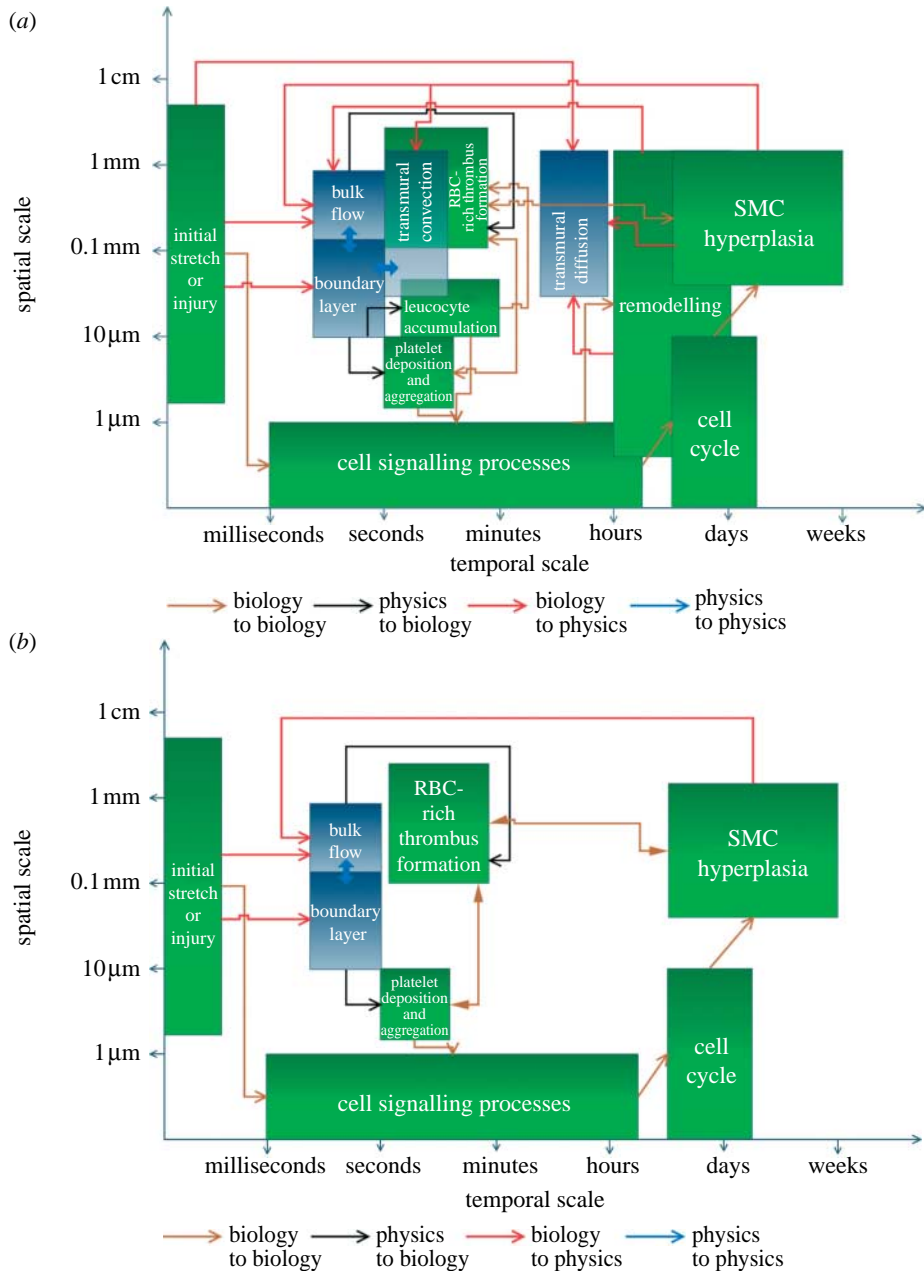
Figure 4. SSMs for ISR. (*a*) Comprehensive SSM for ISR. (*b*) Simplified version of the SSM showing the minimum number of explicitly modelled processes considered necessary for the system model to remain representative.

current time-step, and the simulation can proceed to the next iteration. However, before doing so, an *intermediate* observation operator **O$_i$** computes observables from the state variables f. After termination of the main iteration loop, a *final* observation is made of the state variables with the **O$_f$** operator.

Depending on the interaction region and other details of the computational domain (a single domain, where both processes act, or multiple domains, where each process has its own subdomain and interaction is along domain boundaries), we can now define the coupling templates. As an example, consider Weinan's heterogeneous multiscale method (Weinan *et al.* 2007). On close inspection, it must be concluded that this is a coupling template for single-domain processes in interaction region 3.1 (i.e. process B now lies in region 3.1 of figure 3*b*). At each time-step of the macroscopic process B, a microscopic process A is initialized using macroscopic information. The microscopic model then runs to completion and sends final information to the collision operator of the macroscopic process. In terms of the SEL of the macroscopic process A and the microscopic process B, we find as coupling template $O_f^B \rightarrow C^A$; $O_i^A \rightarrow f_{init}^B$. It can be demonstrated (Hoekstra *et al.* 2007) that the coupling process reduces to the identification of the points of interaction between two single-scale processes, each represented in terms of the SEL. There are a finite number of interactions between the two processes in the SEL, and these can be catalogued. We refer to the map of interactions as a coupling template. The coupling templates, together with the SSM and the SEL, form the conceptual core of the COAST framework. These templates, in turn, will be available as special classes in the COAST software framework, allowing a quick assembly of a CxA model using the existing single-scale simulations.

5. Development of SSMs for ISR

SSMs were constructed illustrating two levels of complexity. A comprehensive map (figure 4*a*) includes the processes necessary to model drug elution from the stent and its distribution through the vessel wall (i.e. transmural convection and diffusion). This has been simplified to a version consisting of the minimum number of explicitly modelled processes considered necessary for the system model to remain representative of the vessel wall response to injury without consideration of drug elution (figure 4*b*).

The placement of ISR subsystems on the SSM is not an exact science (particularly, given the sometimes qualitative nature of the available data for certain subsystems) and to some degree reflects the extent of the domain that is to be modelled. However, it is not critical that the placement is precise, as the map currently aims only to provide information about how any two processes are separated; if the separation is obvious, then the precise degree of this separation is largely irrelevant at this stage of modelling. Placement is also dependent on the source and the availability of quantitative data, and the particular process of interest. For example, if we consider figure 4*a*, we see that cell signalling processes are lumped into one subsystem, which occurs on a temporal scale of milliseconds to hours and on a sub-micrometre spatial scale. In the context of restenosis, 'cell signalling' could relate to a series of phosphorylation events within an intracellular signalling cascade, which might occur on a temporal scale of the order of milliseconds, or equally it might refer to the transmural diffusion of a cytokine into the vessel wall following release from an EC, which might take place over minutes to hours. The cell signalling processes could therefore be separated further, but for the purposes of the current project, this is not

necessary and we use a 'black box' approach for these elements. Note that such model hierarchies are naturally supported by the CxA approach, and we will take advantage of this where possible.

It is also important to make the distinction between the information contained in figure 2 and that contained in the SSMs (figure 4). For example, although blood flow is relevant throughout the entire time course of ISR, its position on the SSM recognizes that it is only pertinent to model flow over one cardiac cycle. The model would run once before the output is passed to relevant models (e.g. ABM of cells in the arterial wall) that use the data to inform their behaviour, before passing output back to the flow solver, which then takes into account any changes in vessel wall geometry in the following iteration.

For illustration of the way in which process placement on the SSM is determined, consider the process of SMC hyperplasia. SMC hyperplasia refers to the proliferation of VSMCs within the tunica intima to generate neointimal tissue (constituting the restenotic lesion). Several dogmas exist with regard to the origin of these SMCs (see §3); however, it is largely accepted that, once present in the tunica intima, VSMC hyperplasia and deposition of extracellular matrix lead to the generation of a neointimal lesion.

(a) Spatial scale: 30 µm–1.5 mm

It is difficult to define the precise size of a VSMC. Adult VSMCs are not terminally differentiated and may undergo major phenotypic changes in response to environmental stimuli (Fazekas *et al.* 2007). Indeed, VSMCs may exhibit contractile or secretory phenotypes and have been observed to dedifferentiate following vascular injury (Campbell *et al.* 1988; Thyberg *et al.* 1995, 1997). If one considers the contractile phenotype, the cells are spindle shaped and of the order of 80–200 µm long and 5 µm wide, whereas secretory VSMCs are smaller (approx. 30 µm in diameter). The process of VSMC migration from the tunica media to the tunica intima (following arterial injury) is likely to involve distances of approximately 30 µm to 1.5 mm. This value takes into account the thickness of the tunica media and the possibility that the VSMC may originate at the medial/adventitial boundary. In practice, it is more likely that only the innermost layer of the tunica media contains VSMCs capable of migration (Thyberg *et al.* 1997), thus reducing this estimate. In cases of severe vessel injury during stent placement, subsequent neointimal growth can progress to completely occlude the vessel. This therefore places the upper limit for the spatial scale at the upper limit of the lumen radius which, in swine, is of the order of 1.5 mm.

(b) Temporal scale: days to weeks

Cultured porcine aortic SMCs require approximately 32 hours to progress though one cell cycle and divide (Le Breton *et al.* 1996) but the division of one neointimal VSMC alone does not constitute neointimal hyperplasia. It is difficult to define the amount of proliferation that constitutes hyperplasia, and if one assumes that the formation of a neointima requires several rounds of VSMC proliferation, then a spatial scale of days to weeks would seem reasonable.
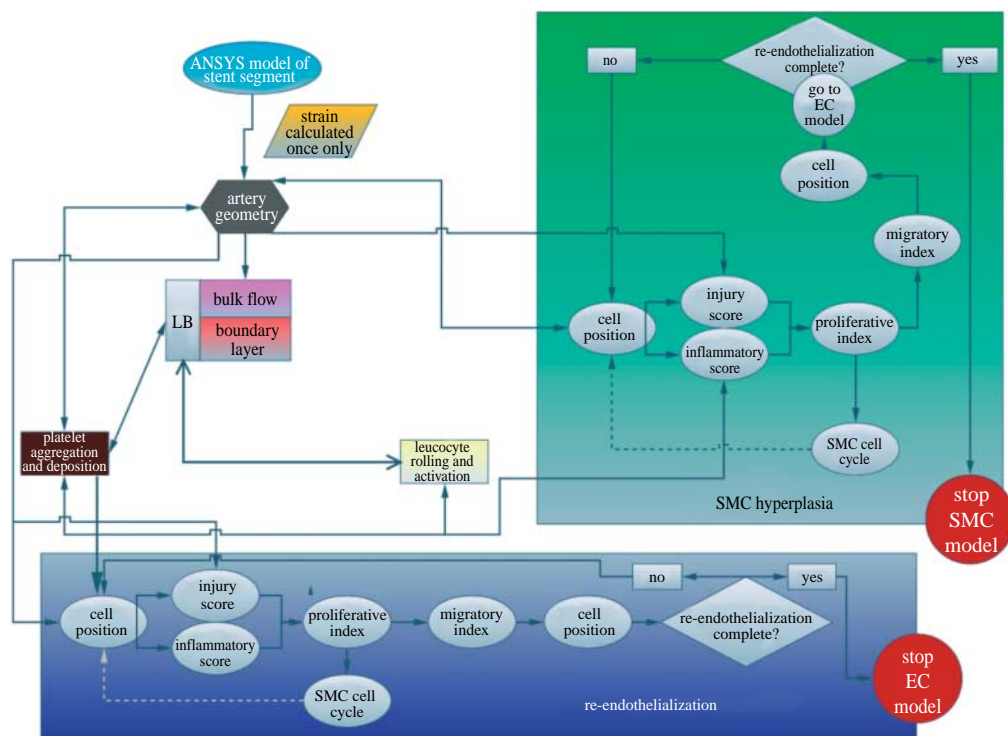
Figure 5. Representation of the interaction algorithm for ISR.

This methodology has proven invaluable as a tool in its own right, stimulating discussion and improving communication between the multidisciplinary team of biologists, clinicians, physicists, engineers and computer scientists involved.

6. The model of ISR

Generation of the SSM allows the individual models necessary to create a functional computational model of ISR to be identified. Figure 5 shows a representation of the interaction algorithm that is based on careful analysis of the processes key to the pathology. A finite-element model (ANSYS) of the stent segment will be used to calculate strain within the initial artery geometry. Description of boundary-layer and bulk flow characteristics will be determined using a lattice Boltzmann solver with mesh refinement (Tölke *et al.* 1998). Information pertaining to flow and geometric characteristics will, in turn, be used to inform models of SMC hyperplasia, EC behaviour and platelet aggregation and deposition. Figure 6 illustrates the output of three of these single-scale models.

Smooth muscle hyperplasia plays a crucial role in the generation of the restenotic lesion. It is the migration and proliferation of SMCs that are central to the embodiment of the neointimal lesion. The behaviour of such a cell type is best described by the use of an ABM. Key concepts in developing the ABM have been drawn from that of the epitheliome (Walker *et al.* 2004). The advantage of the
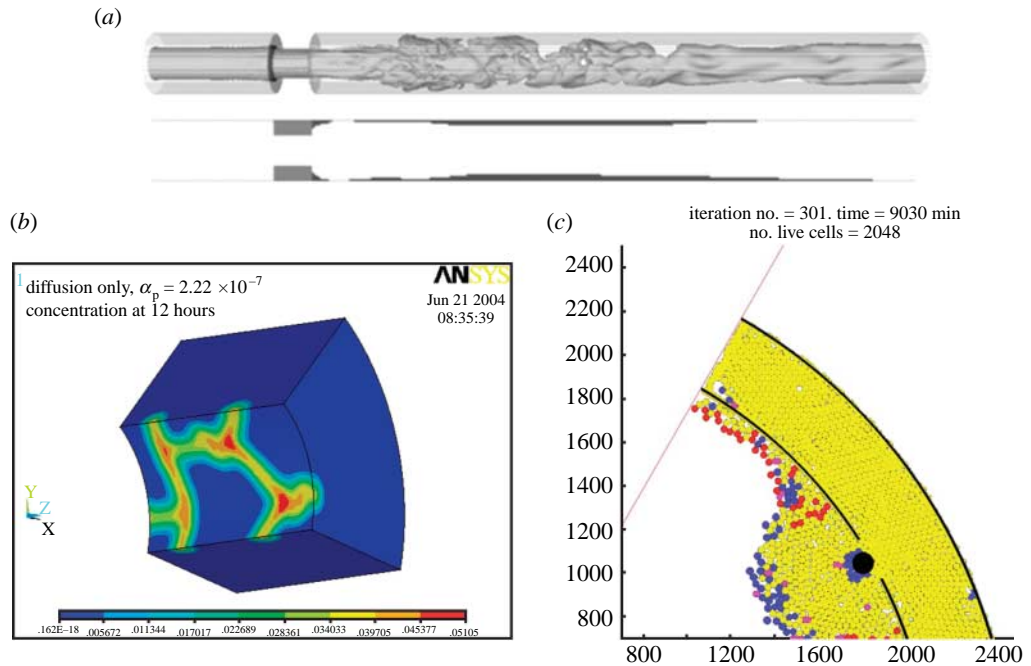
Figure 6. Single-scale models relevant to ISR. (*a*) Lattice Boltzmann flow solution and computed clot distribution in the region of sharp-edged stenosis (Harrison *et al.* 2007). (*b*) Drug elution, convection and diffusion in vessel wall (Hose *et al.* 2004). (*c*) ABM of neointimal growth (COAST).

ABM lies in its inherent capacity for additional layers of complexity as understanding of the behavioural rule sets to which these cells conform progresses. As it is hypothesized that the re-formation of an intact EC layer is crucial in inhibiting ISR, a second class of agents representing individual ECs will be included. The general structure of the ABM developed will be equally transferable to the description of ECs (and to fibroblast and leucocyte behaviour if required).

7. Conclusions

Although there is a wealth of literature on multiscale modelling, almost all focuses on particular applications and very little on formalization of the modelling process, especially in the context of the life sciences. An exception is the comprehensive high-level description presented by Bassingthwaighte *et al.* (2006), which includes a review of strategies and tactics for adaptive multiscale modelling together with important cautionary notes on model reductions, adaptive model modification and related error propagation while confirming that multiscale and multilevel systems modelling is in its infancy.

The current paper describes a methodology for approaching the representation of a complex multiscience, multiscale process in a form that is tractable for computational modelling. The approach is based on three concepts, namely an SSM, a generic sub-execution loop and a coupling template. It is demonstrated

that this approach can be used to construct an algorithmic description of a challenging, clinically important application at the interface between physics and biology, that of ISR. An interesting observation is that the biologists and clinicians working on the development of the SSM describing the process found it to be a very useful conceptual tool for arranging, cataloguing and formalizing the existing knowledge, and indeed for identifying gaps in the current knowledge base and thus informing future experiments. We conclude that this methodology provides a coherent basis for the generation of complex multiscale models (termed CxA) featuring generalized representations of both CA and ABMs.

References

Bassingthwaighte, J. B., Chizeck, H. J. & Atlas, L. 2006 Strategies and tactics in multiscale modeling of cell-to-organ systems. *Proc. IEEE* **94**, 819–831. (doi:10.1109/JPROC.2006.871775)

BCIS 2007 British Cardiovascular Intervention Society. See http://www.bcis.org.uk/.

Bernstein, A., Hing, E., Moss, A., Allen, K., Siller, A. & Tiggle, R. 2003 *Health care in America: trends in utilization.* Hyattsville, MD: National Center for Health Statistics.

BHF 2007 British Heart Foundation Statistics. See http://www.heartstats.org/homepage.asp.

Bienvenu, J.-G., Tanguay, J. F., Chauvet, P. & Merhi, Y. 2001 Relationship between platelets and neutrophil adhesion and neointimal growth after repeated arterial wall injury induced by angioplasty in pigs. *J. Vasc. Res.* **38**, 153–162. (doi:10.1159/000051042)

Campbell, G. R., Campbell, J. H., Manderson, J. A., Horrigan, S. & Rennick, R. E. 1988 Arterial smooth muscle. A multifunctional mesenchymal cell. *Arch. Pathol. Lab. Med.* **112**, 977–986.

Carlsson, J., von Wagenheim, B., Linder, R., Anwari, T. M., Qvist, J., Petersson, I., Magounakis, T. & Lagerqvist, B. 2006 Is late stent thrombosis in drug-eluting stents a real clinical issue? a single-center experience and review of the literature. *Clin. Res. Cardiol.* **96**, 86–93. (doi:10.1007/s00392-007-0464-x)

Dean, C. J., Morton, A. C., Arnold, N. D., Hose, D. R., Crossman, D. C. & Gunn, J. 2005 Relative importance of the components of stent geometry to stretch induced in-stent neointima formation. *Heart* **91**, 1603–1604. (doi:10.1136/hrt.2004.047050)

Di Ventura, B., Lemerle, C., Michalodimitrakis, K. & Serrano, L. 2006 From *in vivo* to *in silico* biology and back. *Nature* **443**, 527–533. (doi:10.1038/nature05127)

Eisenberg, M. J., Ryan, J. & Cohen, D. J. 2006 Drug-eluting stents: the price is not right. *Circulation* **114**, 1745–1754. (doi:10.1161/CIRCULATIONAHA.106.646190)

Farb, A., Sangiorgi, G., Carter, A. J., Walley, V. M., Edwards, W. D., Schwartz, R. S. & Virmani, R. 1999 Pathology of acute and chronic coronary stenting in humans. *Circulation* **99**, 44–52.

Fazekas, C., Kozmann, G. & Hangos, K. M. 2007 Multiscale modeling and time-scale analysis of a human limb. *Multiscale Model. Simul.* **6**, 761–791. (doi:10.1137/060665440)

Finkelstein, A., Hetherington, J., Li, L., Margoninski, O., Saffrey, P., Seymour, R. & Warner, A. 2004 Computational challenges of systems biology. *IEEE Comput.* **37**, 26–33. (doi:10.1109/MC.2004.1297236)

Forrester, J. S., Fishbein, M., Helfant, R. & Fagin, J. 1991 A paradigm for restenosis based on cell biology: clues for the development of new preventive therapies. *J. Am. Coll. Cardiol.* **17**, 758–769.

Ge, J., Shen, C., Liang, C., Chen, L., Qian, J. & Chen, H. 2006 Elevated matrix metalloproteinase expression after stent implantation is associated with restenosis. *Int. J. Cardiol.* **112**, 85–90. (doi:10.1016/j.ijcard.2005.10.016)

Goncharova, E. A., Ammit, A. J., Irani, C., Carroll, R. G., Eszterhas, A. J., Panettieri, R. A. & Krymskaya, V. P. 2002 PI3K is required for proliferation and migration of human pulmonary vascular smooth muscle cells. *Am. J. Physiol. Lung Cell. Mol. Physiol.* **283**, L354–L363. (doi:10.1152/ajplung.00010.2002)

Grimm, V. *et al.* 2005 Pattern-oriented modeling of agent-based complex systems: lessons from ecology. *Science* **310**, 987–991. (doi:10.1126/science.1116681)

Haga, J. H., Li, Y. S. & Chien, S. 2007 Molecular basis of the effects of mechanical stretch on vascular smooth muscle cells. *J. Biomech.* **40**, 947–960. (doi:10.1016/j.jbiomech.2006.04.011)

Harrison, S. E., Smith, S. M., Bernsdorf, J., Hose, D. R. & Lawford, P. V. 2007 Application and validation of the lattice Boltzmann method for modelling flow-related clotting. *J. Biomech.* **40**, 3023–3028. (doi:10.1016/j.jbiomech.2007.01.026)

Hoekstra, A., Lorenz, E., Falcone, J. & Chopard, B. 2007 Towards a complex automata framework for multi-scale modeling: formalism and the scale separation map. *Int. J. Multiscale Comp. Eng.* **5**, 491–502. (doi:10.1615/IntJMultCompEng.v5.i6.60)

Hose, D., Narracott, A., Griffiths, B., Mahmood, S., Gunn, J., Sweeney, D. & Lawford, P. 2004 A thermal analogy for modelling drug elution from cardiovascular stents. *Comput. Methods Biomech. Biomed. Eng.* **7**, 257–264. (doi:10.1080/10255840412331303140)

Hunter, P. & Nielson, P. 2005 A strategy for integrated computational physiology. *Physiology* **20**, 316–325. (doi:10.1152/physiol.00022.2005)

Hunter, P. J., Li, W. W., McCulloch, A. D. & Noble, D. 2006 Multiscale modeling: physiome project standards, tools, and databases. *IEEE Comput.* **39**, 48–54. (doi:10.1109/MC.2006.392)

Ilachinski, A. 2001 *Cellular automata: a discrete universe.* Singapore: World Scientific.

Indolfi, C., Mongiardo, A., Curcio, A. & Torella, D. 2003 Molecular mechanisms of in-stent restenosis and approach to therapy with eluting stents. *Trends Cardiovasc. Med.* **13**, 142–148. (doi:10.1016/S1050-1738(03)00038-0)

Ingram, G., Cameron, I. & Hangos, K. 2004 Classification and analysis of integrating frameworks in multiscale modelling. *Chem. Eng. Sci.* **59**, 2171–2187. (doi:10.1016/j.ces.2004.02.010)

Klurfeld, D. M. 1985 Identification of foam cells in human atherosclerotic lesions as macrophages using monoclonal antibodies. *Arch. Pathol. Lab. Med.* **109**, 445–449.

Le Breton, H., Plow, E. F. & Topol, E. J. 1996 Role of platelets in restenosis after percutaneous coronary revascularization. *J. Am. Coll. Cardiol.* **28**, 1643–1651. (doi:10.1016/S0735-1097(96)00417-2)

Leon, M. & Stone, G. 2006 In *Presentation at TCT, 25 October 2006.* See www.tctmd.com/csportal/appmanager/tctmd/main?_nfpb=true&_pageLabel=TCTMDContent&hdCon=1453648.

Malik, N., Gunn, J., Holt, C. M., Shepherd, L., Francis, S. E., Newman, C. M., Crossman, D. C. & Cumberland, D. C. 1998 Intravascular stents: a new technique for tissue processing for histology, immunohistochemistry, and transmission electron microscopy. *Heart* **80**, 509–516.

Masselot, A. & Chopard, B. 1998 A lattice Boltzmann model for particle transport and deposition. *Europhys. Lett.* **42**, 259–262. (doi:10.1209/epl/i1998-00239-3)

Merks, R., Hoekstra, A., Kaandorp, J. & Sloot, P. 2003 Models of coral growth: spontaneous branching, compactification and the Laplacian growth assumption. *J. Theor. Biol.* **224**, 153–166. (doi:10.1016/S0022-5193(03)00140-1)

Morton, A. C., Crossman, D. & Gunn, J. 2004 The influence of physical stent parameters upon restenosis. *Pathol. Biol. (Paris)* **52**, 196–205. (doi:10.1016/j.patbio.2004.03.013)

Mudra, H., Regar, E., Klauss, V., Werner, F., Henneke, K. H., Sbarouni, E. & Theisen, K. 1997 Serial follow-up after optimized ultrasound-guided deployment of Palmaz–Schatz stents. In-stent neointimal proliferation without significant reference segment response. *Circulation* **95**, 363–370.

Napoli, C., D'Armiento, F. P., Mancini, F. P., Postiglione, A., Witztum, J. L., Palumbo, G. & Palinski, W. 1997 Fatty streak formation occurs in human fetal aortas and is greatly enhanced by maternal hypercholesterolemia. *J. Clin. Invest.* **100**, 2680–2690. (doi:10.1172/JCI119813)

Noble, D. 2002 Modeling the heart—from genes to cells to the whole organ. *Science* **295**, 1678–1682. (doi:10.1126/science.1069881)

OECD 2007 Organisation for Economic Co-operation and Development. See http://www.oecd.org.

Parfyonova, Y., Plekhanova, O., Solomatina, M., Naumov, V., Bobik, A., Berk, B. & Tkachuk, V. 2004 Contrasting effects of urokinase and tissue-type plasminogen activators on neointima formation and vessel remodelling after arterial injury. *J. Vasc. Res.* **41**, 268–276. (doi:10.1159/000078825)

Quarteroni, A. & Veneziani, A. 2003 Analysis of a geometrical multiscale model based on the coupling of ODEs and PDEs for blood flow simulations. *Multiscale Model. Simul.* **1**, 173–195. (doi:10.1137/S1540345902408482)

Sata, M. 2003 Circulating vascular progenitor cells contribute to vascular repair, remodeling, and lesion formation. *Trends Cardiovasc. Med.* **13**, 249–253. (doi:10.1016/S1050-1738(03)00106-3)

Sloot, P., Tirado-Ramos, A., Altintas, I., Bubak, M. & Boucher, C. 2006 From molecule to man: decision support in individualized E-health. *Computer* **39**, 40–46. (doi:10.1109/MC.2006.380)

Smye, S. W. & Clayton, R. H. 2002 Mathematical modelling for the new millenium: medicine by numbers. *Med. Eng. Phys.* **24**, 565–574. (doi:10.1016/S1350-4533(02)00049-8)

Tezduyar, T., Sathe, S., Cragin, T., Nanna, B., Conklin, B., Pausewang, J. & Schwaab, M. 2007 Modelling of fluid–structure interactions with the space-time finite elements: arterial fluid mechanics. *Int. J. Numer. Methods Fluids* **54**, 901–922. (doi:10.1002/fld.1443)

Thyberg, J., Blomgren, K., Hedin, U. & Dryjski, M. 1995 Phenotypic modulation of smooth muscle cells during the formation of neointimal thickenings in the rat carotid artery after balloon injury: an electron-microscopic and stereological study. *Cell Tissue Res.* **281**, 421–433. (doi:10.1007/BF00417860)

Thyberg, J., Blomgren, K., Roy, J., Tran, P. K. & Hedin, U. 1997 Phenotypic modulation of smooth muscle cells after arterial injury is associated with changes in the distribution of laminin and fibronectin. *J. Histochem. Cytochem.* **45**, 837–846.

Tölke, J., Krafczyk, M., Schulz, M., Rank, E. & Berrios, R. 1998 Implicit discretization and non-uniform mesh refinement approaches for FD discretizations of LBGK models. *Int. J. Mod. Phys. C* **9**, 1143–1157. (doi:10.1142/S0129183198001059)

Walker, D. C., Southgate, J., Hill, G., Holcombe, M., Hose, D. R., Wood, S. M., Mac Neil, S. & Smallwood, R. H. 2004 The epitheliome: agent-based modelling of the social behaviour of cells. *Biosystems* **76**, 89–100. (doi:10.1016/j.biosystems.2004.05.025)

Weinan, E., Engquist, B., Li, X., Ren, W. & Vanden-Eijnden, E. 2007 Heterogeneous multiscale methods: a review. *Commun. Comput. Phys.* **2**, 367–450.

Welt, F. G. P. & Rogers, C. 2002 Inflammation and restenosis in the stent era. *Arterioscler. Thromb. Vasc. Biol.* **22**, 1769–1776. (doi:10.1161/01.ATV.0000037100.44766.5B)

Wooldridge, M. 2002 *Introduction to multiagent systems.* New York, NY: Wiley.

Yokoyama, S., Ikeda, H., Haramaki, N., Yasukawa, H., Murohara, T. & Imaizumi, T. 2005 Platelet P-selectin plays an important role in arterial thrombogenesis by forming large stable platelet–leukocyte aggregates. *J. Am. Coll. Cardiol.* **45**, 1280–1286. (doi:10.1016/j.jacc.2004.12.071)

Zalewski, A., Shi, Y. & Johnson, A. G. 2002 Diverse origin of intimal cells: smooth muscle cells, myofibroblasts, fibroblasts, and beyond? *Circ. Res.* **91**, 652–655. (doi:10.1161/01.RES.0000038996.97287.9A)

Zhou, R. H., Lee, T. S., Tsou, T. C., Rannou, F., Li, Y. S., Chien, S. & Shyy, J. Y. 2003 Stent implantation activates Akt in the vessel wall: role of mechanical stretch in vascular smooth muscle cells. *Arterioscler. Thromb. Vasc. Biol.* **23**, 2015–2020. (doi:10.1161/01.ATV.0000095161.06906.ED)